35th International Electric Vehicle Symposium and Exhibition (EVS35)
Oslo, Norway, June 11-15, 2022

Strategy beats power: Cooling system design for battery-electric long-haul trucks

Olaf Teichert[1], Jakob Schneider[1], Markus Lienkamp[1]
[1]*Olaf Teichert (corresponding author), Technical University of Munich, School of Engineering & Design, Institute of Automotive Technology, 85748 Garching, Germany, olaf.teichert@tum.de*

Executive Summary

Sizing a battery thermal management system (BTMS) for worst-case scenarios ensures that the battery is always operated in the preferred temperature window, but requires large, heavy, expensive cooling systems, and may cause large temperature differences within and between the cells. A control strategy that activates the cooling system at low cell temperatures minimizes battery aging, but also increases the cooling system energy consumption. To find the optimal installed cooling power and control strategy, we apply a previously developed method for the techno-economic design of battery thermal management systems to a battery-electric long-haul truck. Results show that the cost-optimal installed thermal cooling power is $85\,\%$ lower than the peak ohmic losses. The cost-optimal cooling strategy activates the cooling system when the cell temperature exceeds $25\,°\mathrm{C}$, which is lower than the cooling thresholds observed in electric passenger cars. The control strategy has a larger impact on the system cost than the installed cooling power. *Keywords: Truck, LCC (Life Cycle Cost), battery, simulation, thermal management*

1 Introduction

Even though trucks only have a share of $9\,\%$ in the global vehicle fleet, they are responsible for $39\,\%$ of carbon emissions in the transportation sector [1]. In order to reach the targets stipulated in the Paris climate agreement, it is therefore essential to replace conventional diesel powertrains with zero emission alternatives. Battery-electric trucks (BET) offer a potential solution, but still face challenges regarding payload and operating range requirements. Forrest et al. [2] showed that the feasibility of BET improves if fast charging is available. However, fast charging causes increased ohmic losses, which result in higher battery temperatures and reduced battery life.
High battery temperatures can be avoided by installing active cooling, but the cooling system increases the battery volume and mass, causes additional investment and maintenance costs, and increases auxiliary power consumption. The design and control of an active cooling system therefore need to balance the trade-off between cooling system cost and energy consumption on the one hand, and battery aging on the other hand. The impact of different cooling strategies was investigated in previous studies.
Xie et al. [3] developed an MPC-based control strategy for a refrigerant cooling system. Their results show that battery aging could be maintained, while the cooling system energy consumption could be reduced by $24.5\,\%$ compared to an on-off controller.
Pham et al. [4] present a control strategy for a refrigerant-cooling system in a hybrid-electric heavy-duty truck, that reduces the total fuel consumption by $1.8\,\%$ while maintaining a favorable battery temperature.
Although the optimization of the BTMS control was addressed in previous studies, the trade-off between battery aging and energy consumption was not quantified. Furthermore, the impact of the installed cooling power has not been investigated. In this work we show the impact of the installed cooling power and cooling threshold on the total cost of ownership, using a previously developed method for the techno-economic design of battery thermal management systems [5].

2 Method

To determine the impact of the installed cooling power and cooling threshold on the total cost of ownership, we combine a battery simulation with a cost model, as shown in Fig. 1. For a given installed cooling power, cooling threshold and load profile, we use a battery simulation to determine the battery life and cooling system energy consumption. Based on these values, a cost model determines the costs that are influenced by the installed cooling power and cooling threshold: the battery investment costs, BTMS investment costs, and cooling energy consumption costs. The sum of these cost components is referred to as the relevant cost of ownership (RCO). The optimal installed cooling power and cooling threshold correspond to those at which the RCO is minimized.

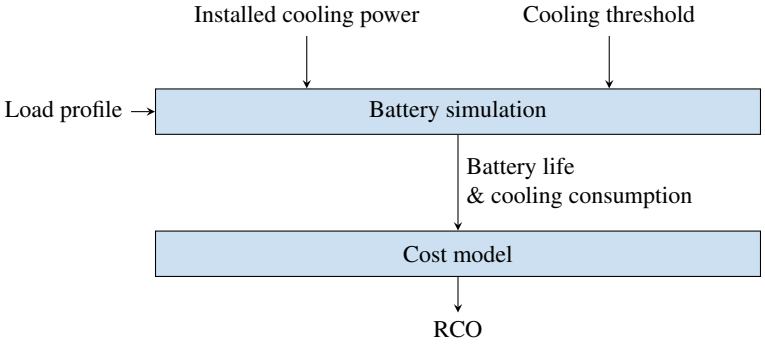

Figure 1: Illustration of the method to determine the optimal installed cooling power and cooling threshold.

2.1 Battery simulation

The battery life and cooling system energy consumption are determined using a battery simulation. For this purpose, we use a battery model that was published in previous work [5] and is shown in Fig. 2. The thermal model was updated to reflect a battery used in a battery-electric truck, while all other sub-models remain unchanged. For the detailed description of the model we refer to [5]. In the following we will give a broad overview of the simulation steps and subsequently describe the changes made to the thermal model.

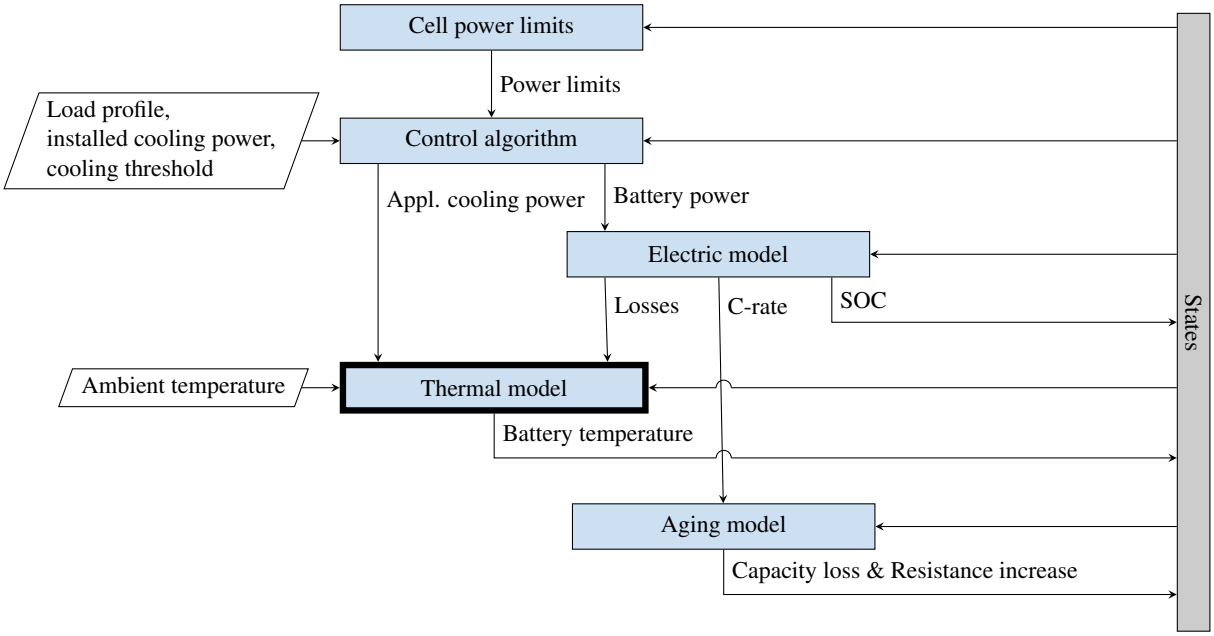

Figure 2: Electric-thermal-aging model used in the battery simulation, adapted from [5]. Inputs are shown as white parallelograms, sub-models as blue rectangles and the system states as a gray rectangle. The only sub-model that was altered in this work is the thermal model, highlighted by a thick border.

At each time step, first the cell power limits are calculated, based on the temperature, SOC and aging state of the cell. Subsequently, a control algorithm determines the applied cooling power and power drawn from or supplied to the battery. The control algorithm uses a simple on-off logic, where the full cooling power is applied if the cell temperature is above the cooling threshold, and no cooling power is applied, if the cell temperature is below the cooling threshold. The electric model determines the ohmic losses, C-rate and SOC for the power drawn from or supplied to the battery. The thermal model updates the battery temperature based on the ohmic losses and applied cooling power. Finally, an aging model updates the aging state of the battery. These steps are repeated until the end of life condition of the battery is reached, which allows modeling the impact of seasonal changes in the ambient temperature and progressing battery degradation.

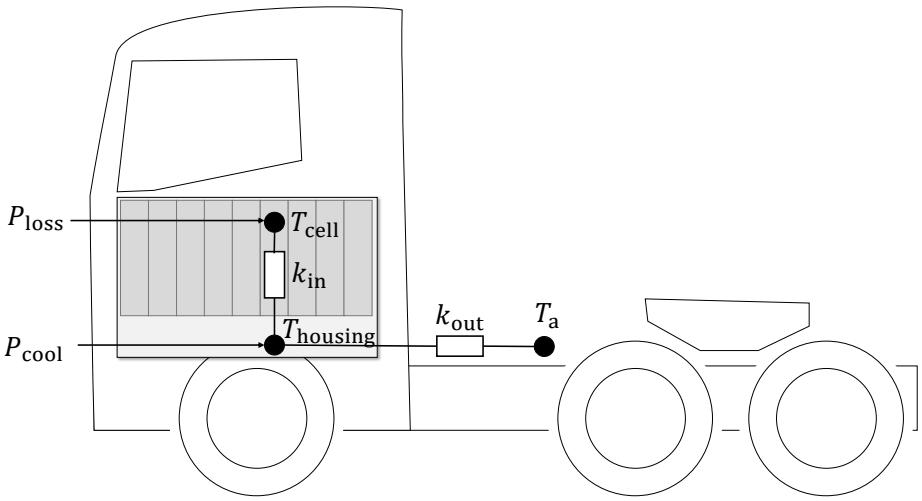

Figure 3: Thermal model of the battery in a battery-electric long-haul truck.

The thermal model was adapted to model the thermal behavior of a battery in a battery-electric truck. The battery temperature is modeled using a lumped-capacitance model with two thermal masses, as shown in Fig. 3. The first thermal mass is the battery housing, whereas the second thermal mass is the cell core. When the battery cooling system is active, heat is directly removed from the battery housing, which approximates the behavior of a battery with integrated cooling channels. Ohmic losses act directly on the cell core. The updated housing and cell temperature at each step are calculated using eq. (1) and (2) respectively, where T_{housing} denotes the housing temperature, k is the timestep index, Δt the timestep duration, P_{cool} the applied cooling power, COP the cooling system coefficient of performance, k_{in} the thermal heat transfer coefficient between the cell core and cell can, n_{cells} the number of cells, T_{cell} the cell temperature, k_{out} the heat transfer coefficient between the housing and ambient, C_{housing} the housing heat capacity, P_{loss} the ohmic losses in a single cell and C_{cell} a cell's heat capacity.

$$T_{\text{housing,k+1}} = T_{\text{housing,k}} + \Delta t \frac{P_{\text{cool}} COP + k_{\text{in}} n_{\text{cells}} (T_{\text{cell,k}} - T_{\text{housing,k}}) + k_{\text{out}} (T_{\text{a}} - T_{\text{housing,k}})}{C_{\text{housing}}} \tag{1}$$

$$T_{\text{cell,k+1}} = T_{\text{cell,k}} + \Delta t \frac{P_{\text{loss}} + k_{\text{in}} (T_{\text{housing,k}} - T_{\text{cell,k}})}{C_{\text{cell}}} \tag{2}$$

2.2 Cost model

The cost model considers only the cost components that are affected by the installed cooling power or cooling threshold. In order to compare capital and operating expenses, the capital costs are expressed by their annual discounted depreciation. The RCO is then given by eq. (3), where C_{bat} describes the annual discounted depreciation of the battery, C_{BTMS} the annual discounted depreciation of the cooling system and C_{ene} the annual cooling energy consumption costs.

$$\text{RCO} = C_{\text{bat}} + C_{\text{BTMS}} + C_{\text{ene}} \tag{3}$$

The annual discounted battery depreciation is given by eq. (4), where c_{bat} is the specific battery cost, E_{bat} the battery size, r the discount rate and t_{bat} the battery life. The fraction term is the capital recovery factor that converts the investment into the annual discounted depreciation.

$$C_{\text{bat}} = c_{\text{bat}} E_{\text{bat}} \frac{(1-r)\, r^{t_{\text{bat}}}}{r^{t_{\text{bat}}} - 1} \tag{4}$$

The annual discounted depreciation of the installed cooling system is calculated using eq. 5, where c_{BTMS} is the specific investment cost, P_{cooler} the installed cooling power and t_{BTMS} the BTMS lifetime.

$$C_{\text{BTMS}} = c_{\text{BTMS}} P_{\text{cooler}} \frac{(1-r)\, r^{t_{\text{BTMS}}}}{r^{t_{\text{BTMS}}} - 1} \tag{5}$$

Finally, the annual cooling system energy consumption costs are calculated by eq. (6), where c_{elec} is the electricity cost and E_{cool} the annual cooling consumption.

$$C_{\text{ene}} = c_{\text{elec}} E_{\text{cool}} \tag{6}$$

3 Implementation

The optimal cooling threshold and installed cooling power are determined for a BET operating in Germany. The ambient temperature profile corresponds to hourly recordings for the year 2015 in Munich, Germany [6].
The power demand during driving was simulated using a distance-based quasi-static longitudinal dynamics simulation based on the VECTO long-haul driving cycle. For a detailed description of the vehicle model and parameters we refer to [7]. The simulated power profile was concatenated to create a weekly repeating load profile, where the truck drives two $4.5\,\text{h}$ trips separated by a $45\,\text{min}$ charging break on Monday, two $3\,\text{h}$ trips with a $45\,\text{min}$ charging break on Tuesday and Wednesday, and a single $4\,\text{h}$ trip on Thursday and Friday. The total weekly driving duration results in an annual mileage of approximately $120\,000\,\text{km}$, which is slightly higher than the annual mileage of $116\,000\,\text{km}$ used by the European commission to simulate typical truck emissions [8]. The truck has access to $700\,\text{kW}$ during the charging break and $50\,\text{kW}$ overnight.
The battery model uses the parametrization by Schmalstieg et al. [9] that was scaled to reflect the cycle life of status quo automotive batteries [10]. The required battery size of the truck to operate without any limitations until the battery end of life was iteratively determined to be $718\,\text{kWh}$ battery.
The parameters used in the cost model and the adapted thermal model are summarized in Table 1. The cell heat capacity and heat transfer between the cell core and the housing matches that of a $50\,\text{Ah}$ prismatic cell. The number of cells corresponds to the amount required to reach the energy content. The heat transfer coefficient between the housing and ambient was scaled from a previous study that found a heat transfer of $4.343\,\text{W}\,\text{K}^{-1}$ for a $22.1\,\text{kWh}$ [11], assuming that the heat transfer coefficient scales linearly with the external surface area of the battery, and the energy content scales linearly with the volume. The heat capacity of the housing was estimated by assuming that the specific heat capacity of the housing components matches that of aluminum and determining the housing components mass based on the average gravimetric packaging efficiency of a car battery [12]. The specific battery cost corresponds to the status quo for automotive applications. The investment costs and lifetime of the cooling system match those of a stationary heat pump. The electricity cost correspond to the industry tarif 2021 in Germany.

Table 1: Usecase parameters

	Parameter	Symbol	Value
Thermal model	Number of cells	n_{cells}	3989
	Heat capacity cell	C_{cell}	$60.2\,\text{J}\,\text{K}^{-1}$ [13]
	Heat transfer coefficient cell core to housing	k_{in}	$0.23\,\text{W}\,\text{K}^{-1}$ [13]
	Heat transfer coefficient housing to ambient	k_{out}	$44.2\,\text{W}\,\text{K}^{-1}$
	Heat capacity housing	C_{housing}	$3.15\,\text{MJ}\,\text{K}^{-1}$
	Coefficient of Performance	COP	-3 [14]
Cost model	Discount rate	r	1.05 [15]
	Specific battery cost	c_{bat}	€$157\,\text{kWh}^{-1}$ [16]
	Specific cooling system investment costs	c_{BTMS}	€$1\,\text{W}^{-1}$ [17]
	Cooler lifetime	t_{BTMS}	$20\,\text{year}$ [17]
	Electricity cost	c_{elec}	€$0.1909\,\text{kWh}^{-1}$ [18]

4 Results

The top pane of Fig. 4 shows the power drawn from and supplied to the battery. The resulting cell temperatures for different installed cooling powers and a cooling threshold of 25 °C are shown in the lower pane. The peak ohmic losses are 58.9 kW on pack level. With a COP of 3, the 20 kW cooling system is able to maintain the cell temperature below 25 °C at all times. With the 3 kW cooling system, the cell temperature increases during the fast-charging event and is only reduced to the target temperature during subsequent operation. The highest cell temperatures are reached by the passively cooled system. Fig. 5 shows the battery operation for the same installed cooling powers and cooling threshold over a full year. The results show that high temperatures are mainly reached in summer, whereas in winter low ambient temperatures prevent overheating the battery.

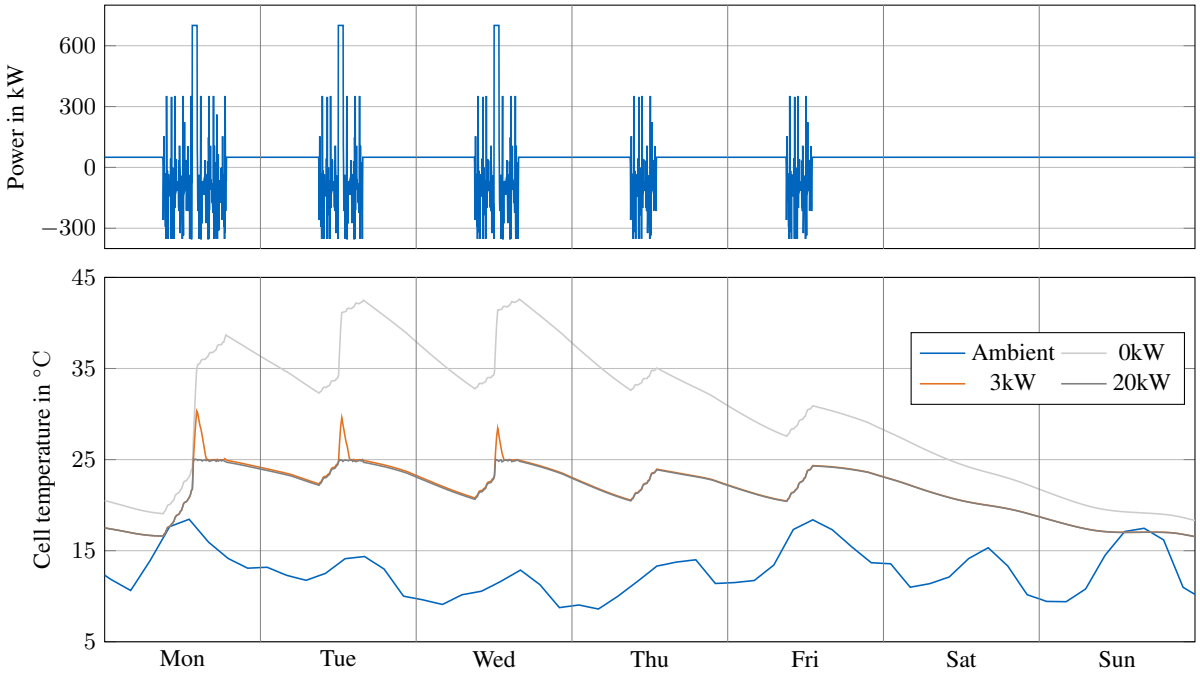

Figure 4: Power demand of a truck charged with 700 kW and cell temperature for three installed cooling powers at a cooling threshold of 25 °C.

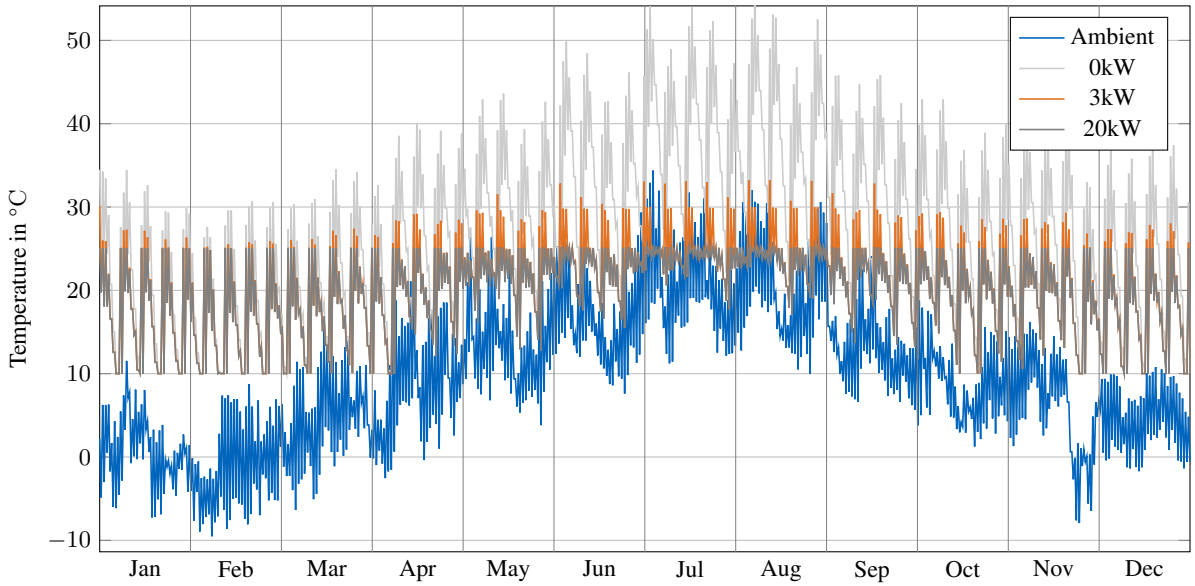

Figure 5: Cell temperatures throughout a year of operation in Munich for different installed cooling powers

Fig. 6 shows operation and cost parameters for a range of installed cooling powers and cooling thresholds. The cost-optimal configuration is marked by a red dot and corresponds to an installed cooling power of $3\,\mathrm{kW}$ and a cooling threshold of $25\,^{\circ}\mathrm{C}$. The top-left pane shows that the maximum cell temperature decreases as the installed cooling power is increased and the cooling threshold is decreased. High cooling powers are able to remove heat quickly, while activating the cooling system at low temperatures avoids high temperatures. The top-right pane shows that the average cell temperature decreases as the installed cooling power is increased and the cooling threshold is decreased. However, the impact of the installed cooling power on the average temperature is smaller than the impact on the maximum cell temperature, since the higher cooling powers are only required during the infrequent fast charging events. The left pane in the second row shows that the maximum temperature inhomogenity within the cells increases as the installed cooling power increases. This is caused by the thermal resistance between the cell core, where the ohmic losses are generated, and the housing, where heat is removed by the cooling system. The temperature inhomogenities are slightly higher at low cooling thresholds since the internal resistance of the cell decreases at higher temperatures, thereby reducing ohmic losses. The right pane in the second row shows that the impact of the installed cooling power and cooling threshold on the battery life closely follows the impact on the average temperature. The cooling threshold has a larger impact on the battery life than the installed cooling power. The third-row left pane shows the resulting impact on the annual battery depreciation. The battery depreciation costs depend on the battery life and therefore decrease with higher installed cooling powers and lower cooling thresholds. However, the impact of the installed cooling power is minor. The third-row right pane shows how the BTMS depreciation increases for higher installed cooling powers, whereas it is independent of the cooling threshold. The energy consumption costs, shown in the bottom left panel, increase with higher cooling thresholds and installed cooling powers, following the trend seen for the average temperature. Finally, the bottom right pane shows the RCO. The higher battery life achieved at lower cooling thresholds outweighs the higher energy costs, resulting in an optimal cooling threshold of $25\,^{\circ}\mathrm{C}$. The optimal installed cooling power of $3\,\mathrm{kW}$ minimizes the trade-off of between the higher BTMS costs and the lower battery costs due to the prolonged battery life.

5 Discussion & Conclusion

We investigated the impact of the installed cooling power and the cooling threshold on the system cost of a battery-electric truck. The results show that the cost-optimal installed cooling power is $15\,\%$ of peak ohmic losses. Although, the achievable reduction in BTMS investment costs is small compared to the battery cost, down-sizing the installed cooling power also leads to other benefits, such as reductions in weight, volume and operating noise, or secondary effects such as lower consumption and increased payload capability. The cost-optimal cooling strategy activates the cooling system when the cell temperature exceeds $25\,^{\circ}\mathrm{C}$. This is lower than the cooling thresholds of $32.5\,^{\circ}\mathrm{C}$ observed in a VW ID.3 [10].
Although we took great care in parametrizing our battery model, the following limitations should be noted. First, due to the limited availability of electric-thermal-aging battery models, we had to scale a fully-parametrized but outdated model to approximate the cycle life of status quo cells. This shows the importance of the availability of up-to-date aging models. Second, charging powers are expected to increase in the future. To avoid reduced charging power at cold temperature, heating may be required. In future work, we plan to use our modular simulation framework to find the optimal combination of heating and battery insulation. Finally, the used lumped capacitance model is not able to model the impact of temperature inhomogenities within the battery pack. A homogeneous temperature distribution within the battery pack is important, because the lifetime of a battery is determined by the cell with the highest degradation. The BTMS therefore needs to minimze the thermal inhomogenities in the system. In future work, we plan to quantify the impact of reducing the temperature distribution within a battery pack on the system costs.

Acknowledgments

The work of O.T. was sponsored by the Federal Ministry of Education and Research Germany within the project "BetterBat" under grant number 03XP0362C. The work of J.S. was sponsored by the Federal Ministry for Economic Affairs and Energy Germany within the project "NEFTON" under grant number 01MV21004A.

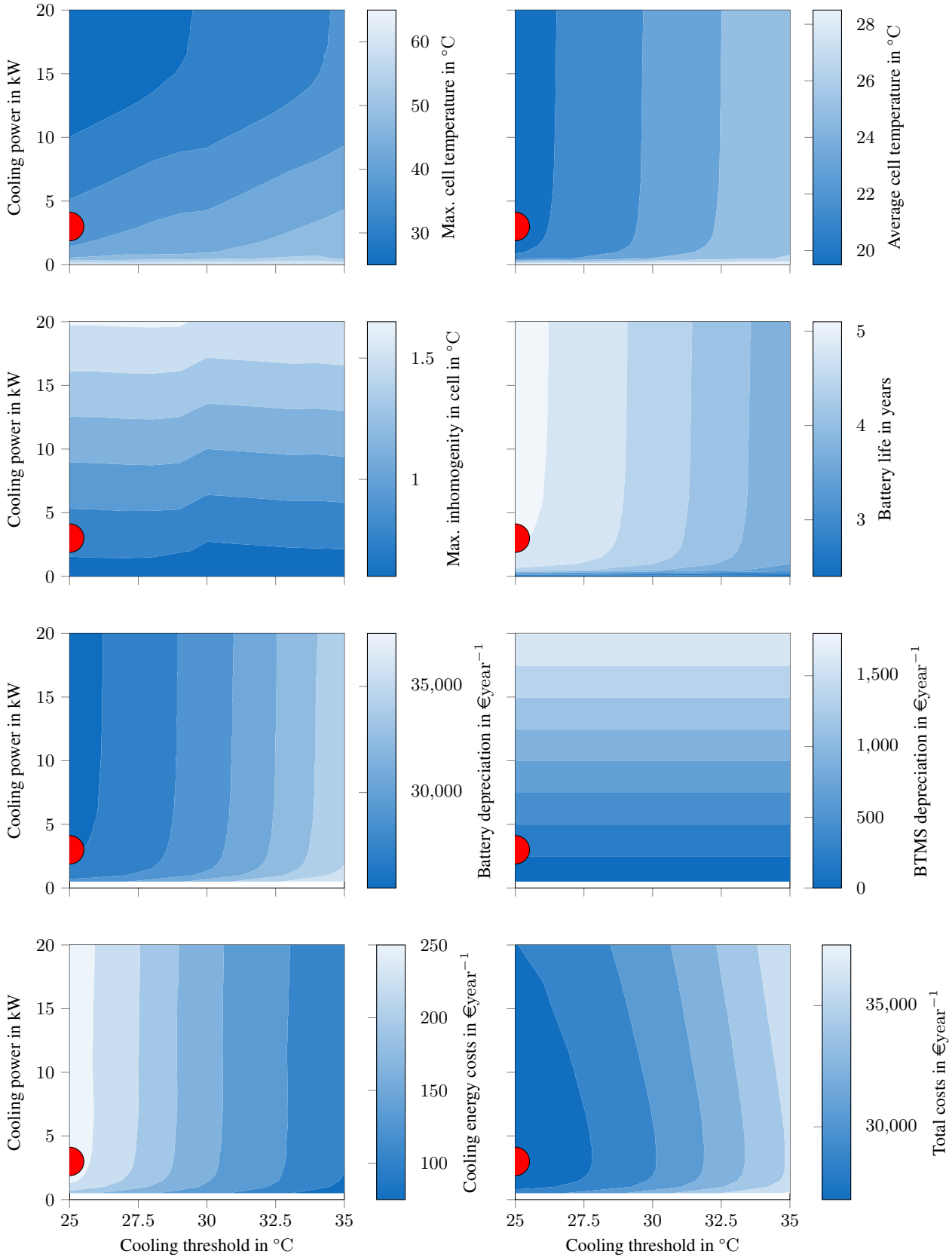

Figure 6: Battery operation and cost components.

References

[1] M. Moultak, N. Lutsey, and D. Hall, "Transitioning to zero-emission heavy-duty freight vehicles," *Int. Counc. Clean Transp*, 2017.

[2] K. Forrest, M. Mac Kinnon, B. Tarroja, and S. Samuelsen, "Estimating the technical feasibility of fuel cell and battery electric vehicles for the medium and heavy duty sectors in california," *Applied Energy*, vol. 276, p. 115439, 2020.

[3] Y. Xie, C. Wang, X. Hu, X. Lin, Y. Zhang, and W. Li, "An mpc-based control strategy for electric vehicle battery cooling considering energy saving and battery lifespan," *IEEE Transactions on Vehicular Technology*, vol. 69, no. 12, pp. 14 657–14 673, 2020.

[4] T. Pham, J. T. Kessels, P. Van den Bosch, R. G. Huisman, and R. Nevels, "On-line energy and battery thermal management for hybrid electric heavy-duty truck," in *2013 American Control Conference*. IEEE, 2013, pp. 710–715.

[5] O. Teichert, F. Müller, and M. Lienkamp, "Techno-economic design of battery thermal management systems in different climates," *Journal of Energy Storage*, vol. 48, p. 103832, 2022.

[6] T. Huld, R. Müller, and A. Gambardella, "A new solar radiation database for estimating pv performance in europe and africa," *Solar Energy*, vol. 86, no. 6, pp. 1803–1815, 2012.

[7] O. Teichert, S. Link, J. Schneider, S. Wolff, and M. Lienkamp, "Techno-economic cell selection for battery-electric long-haul trucks," *eTransportation*, 2022, UNDER REVIEW.

[8] The European Parliament and The Council, "Regulation (eu) 2019 / setting co2 emission performance standards for new heavy-duty vehicles and amending regulations (ec) no 595/2009 and (eu) 2018/956 of the european parliament and of the council and council directive 96/53/ec," 2019.

[9] J. Schmalstieg, S. Käbitz, M. Ecker, and D. U. Sauer, "A holistic aging model for li (nimnco) o2 based 18650 lithium-ion batteries," *Journal of Power Sources*, vol. 257, pp. 325–334, 2014.

[10] N. Wassiliadis, M. Steinsträter, M. Schreiber, P. Rosner, L. Nicoletti, F. Schmid, M. Ank, O. Teichert, L. Wildfeuer, J. Schneider *et al.*, "Quantifying the state of the art of electric powertrains in battery electric vehicles: Range, efficiency, and lifetime from component to system level of the volkswagen id. 3," *eTransportation*, p. 100167, 2022.

[11] J. Neubauer and E. Wood, "Thru-life impacts of driver aggression, climate, cabin thermal management, and battery thermal management on battery electric vehicle utility," *Journal of Power Sources*, vol. 259, pp. 262–275, 2014.

[12] H. Löbberding, S. Wessel, C. Offermanns, M. Kehrer, J. Rother, H. Heimes, and A. Kampker, "From cell to battery system in bevs: analysis of system packing efficiency and cell types," *World Electric Vehicle Journal*, vol. 11, no. 4, p. 77, 2020.

[13] X. Cui, J. Zeng, H. Zhang, J. Yang, J. Qiao, J. Li, and W. Li, "Optimization of the lumped parameter thermal model for hard-cased li-ion batteries," *Journal of Energy Storage*, vol. 32, p. 101758, 2020.

[14] M. Schimpe, M. Naumann, N. Truong, H. C. Hesse, S. Santhanagopalan, A. Saxon, and A. Jossen, "Energy efficiency evaluation of a stationary lithium-ion battery container storage system via electro-thermal modeling and detailed component analysis," *Applied energy*, vol. 210, pp. 211–229, 2018.

[15] F. Trocker, O. Teichert, M. Gallet, A. Ongel, and M. Lienkamp, "City-scale assessment of stationary energy storage supporting end-station fast charging for different bus-fleet electrification levels," *Journal of Energy Storage*, vol. 32, p. 101794, 2020.

[16] A. König, L. Nicoletti, D. Schröder, S. Wolff, A. Waclaw, and M. Lienkamp, "An overview of parameter and cost for battery electric vehicles," *World Electric Vehicle Journal*, vol. 12, no. 1, p. 21, 2021.

[17] Danish Energy Agency, "Technology data for energy plants. individual heating plants and energy transport," May 2012.

[18] BDEW, "Strompreisanalyse juni 2021," Jun 2021, https://www.bdew.de/service/daten-und-grafiken/bdew-strompreisanalyse/.

Presenter Biography

Olaf Teichert received a bachelor's in mechanical engineering from Delft University of Technology and a master's in automotive engineering from Technical University of Munich (TUM). He is currently pursuing a Ph.D. degree with the Institute of Automotive Technology at the TUM, where his research focuses on the techno-economic battery design for commercial vehicles including cell selection, joint optimization of battery capacity & charging infrastructure, and the design of the battery thermal management system.

Jakob Schneider received a bachelor's in mechanical engineering and a master's in automotive engineering from the Technical University of Munich (TUM). He is currently pursuing a Ph.D. degree with the Institute of Automotive Technology at TUM. His research focuses on the influence of fast-charging and future battery technologys on the battery system of heavy-duty vehicles as well as the design of the battery thermal management system.

Markus Lienkamp is conducting research in the area of electro-mobility with the objective of developing new vehicle concepts. He is professor of the Institute of Automotive Technology at Technical University of Munich (TUM). After studying mechanical engineering at TU Darmstadt and Cornell University, he obtained his doctorate at TU Darmstadt (1995). He worked at Volkswagen as part of an international trainee program and took part in a joint venture between Ford and Volkswagen in Portugal. Returning to Germany, he led the brake testing department in the VW commercial vehicle development section in Wolfsburg. He later became head of the "Electronics and Vehicle" research department in Volkswagen AG's Group Research division. His main priorities were advanced driver assistance systems and vehicle concepts for electro-mobility. Prof. Lienkamp is heading the Chair of Automotive Technology at TUM since November 2009.